

Anionic Metal–Organic Framework for Adsorption and Separation of Light Hydrocarbons

Jia Li,[†] Hong-Ru Fu,[‡] Jian Zhang,[‡] Lan-Sun Zheng,[†] and Jun Tao^{*,†}[†]State Key Laboratory of Physical Chemistry of Solid Surfaces and Department of Chemistry, College of Chemistry and Chemical Engineering, Xiamen University, Xiamen 361005, People's Republic of China[‡]Fujian Institute of Research on the Structure of Matter, Chinese Academy of Sciences, Fuzhou 350002, People's Republic of China

S Supporting Information

ABSTRACT: The reaction of nickel(II) sulfate with 4,4',4''-s-triazine-2,4,6-triyltribenzoate in dimethyl sulfoxide afforded a hexanuclear nickel(II)-based anionic 2-fold interpenetrated metal–organic framework exhibiting the ability to adsorb and separate light hydrocarbons and canted antiferromagnetism.

Metal–organic frameworks (MOFs) have attracted great interest as a new type of porous material in the past 2 decades.^{1–4} MOFs based on polynuclear units may exhibit not only gas storage/separation but also other physical properties, such as magnetic, nonlinear optical, ferroelectric, and dielectric properties,^{5,6} respectively, thus representing a very interesting and meaningful subject to achieve multifunctional materials.^{7–9}

It has been well-known that the capability of gas uptake is directly proportional to the host–guest interactions and internal surface areas within MOFs. The former has been partly enhanced by modifying bridging ligands with Lewis basic sites, e.g., pyridyl, amino, and hydroxyl groups,¹⁰ or by developing ionic MOFs that possess charge-induced forces.^{11,12} These strategies certainly apply to the design and development of MOFs for adsorbing and separating light hydrocarbons. Light hydrocarbons are very important energy resources in the future, and the prerequisite for their industrial applications is purification. However, the traditional separation technology based on their different boiling points is very energy-intensive. By using MOFs, more environmentally friendly and energy-efficient methods to separate light hydrocarbons may be achieved. Recently, we are using the trigonal-planar ligand 4,4',4''-s-triazine-2,4,6-triyltribenzoate (TATB) to synthesize MOFs, encouraged not only by its known MOF with paddlewheel or μ_3 -O-centered trinuclear units showing high gas uptakes and surface areas¹³ but also by its tendency to encourage π – π interactions between the triazine groups¹⁴ with Lewis basic sites that promote strong interactions between the triazine groups and light hydrocarbon molecules. Here, we report a new MOF, namely, $(\text{H}_3\text{O})_4[\text{Ni}_6(\mu_3\text{-O})_2(\mu_2\text{-OSC}_2\text{H}_6)_2(\text{SO}_4)_2(\text{TATB})_{8/3}]\cdot 4\text{C}_2\text{H}_6\text{O}\cdot 13\text{H}_2\text{O}[(\text{H}_3\text{O})_4\text{I}\cdot\text{S}]$, by using ligand TATB. The anionic framework is built with hexanuclear nickel(II) units and affords a porosity of about 52.4% of the unit cell volume. The framework is 2-fold self-interpenetrated to give an anionic MOF that exhibits high adsorptive selectivity of light hydrocarbons (C_2H_2 , C_2H_4 , and C_2H_6 , respectively, over CH_4) and shows canted antiferromagnetism because of the existence of hexanuclear nickel(II) units.

The title complex was synthesized by a solvothermal method (see the Supporting Information, SI). The framework is negatively charged (see below), which can be compensated for by protonated water molecules.^{14a} The amounts of extraframework solvent molecules were estimated by thermogravimetric (TGA) and elemental analyses (see the SI).

The complex crystallizes in the cubic space group $Im\bar{3}$, and the basic structural unit of framework 1^{4-} is anionic hexanuclear species $[\text{Ni}_6(\mu_3\text{-O})_2(\mu_2\text{-OSC}_2\text{H}_6)_2(\text{CO}_2)_8(\text{SO}_4)_2]^{4-}$, which contains two crystallographically different nickel(II) ions (Figure 1a). The Ni1 ion lies in a distorted octahedral environment,

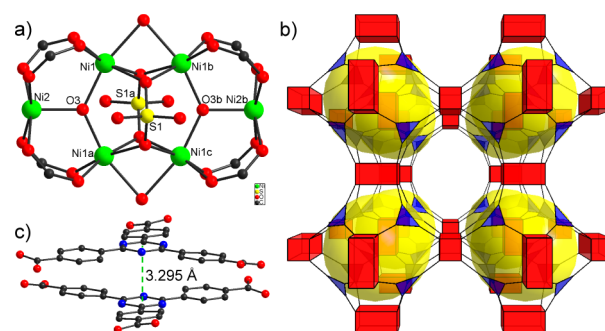


Figure 1. (a) Perspective view of the Ni_6 unit with selective atom labels. Color code: nickel, green; carbon, black; oxygen, red; sulfur, yellow. (b) Topological framework structure viewed along the c axis, where the red cuboid is the Ni_6 unit and the blue triangle is the ligand TATB, respectively. (c) Interligand D_{3d} Peidfort pattern^{14b} observed between two identical (interpenetrated) frameworks in the complex. Guest solvent molecules and hydrogen atoms are omitted for clarity. Symmetry codes: a, $-x, 1 - y, z$; b, $x, 1 - y, -z$; c, $-x, y, -z$.

being coordinated by six oxygen atoms from two carboxylate groups of different TATB ligands, a $\mu_3\text{-O}^{2-}$ ion (O3), a $\mu_2\text{-OSC}_2\text{H}_6$ molecule, and two $\eta^2\text{-}\eta^2\text{-}\mu_4\text{-SO}_4^{2-}$ groups; the Ni2 ion is coordinated by four oxygen atoms from different TATB ligands and one oxygen atom from the $\mu_3\text{-O}^{2-}$ ion (O3), thus forming a square-pyramidal geometry. The structural unit can be viewed as two subunits of trigonal $[\text{Ni}_3(\mu_3\text{-O}^{2-})(\text{CO}_2)_4]^{15}$ bridged by $\eta^2\text{-}\eta^2\text{-}\mu_4\text{-SO}_4^{2-}$ groups and $\mu_2\text{-OSC}_2\text{H}_6$ molecules, and in each subunit, the Ni–O bond lengths range from 1.956(8) to 2.189(5) Å and the three nickel(II) ions are absolutely coplanar (Table S2 in the SI). From a topological point of view, each

Received: February 9, 2015

Published: March 24, 2015



cuboidal $[\text{Ni}_6(\mu_3\text{-O})_2(\mu_2\text{-OSC}_2\text{H}_6)_2(\text{CO}_2)_8(\text{SO}_4)_2]^{4-}$ unit is connected to eight trigonal TATB ligands, and each trigonal TATB ligand, in turn, links three cuboidal units, thus forming a 3,8-connected 3D framework (Figure 1b) that is highly similar to that of a cobalt 1,3,5-benzenetribenzoate MOF reported by us.^{13d} Such a framework is doubly self-interpenetrated (Figure S1 in the SI), generating interframework TATB pairs (Figure 1c) with π - π interactions similar to those reported in TATB MOFs.^{13,14} The triazine rings of each TATB pair are stacked in a highly symmetric face-to-face arrangement (D_{3d} pattern^{14b}) with a centroid-to-centroid distance of 3.295 Å (Figure 1c).

TGA of $(\text{H}_3\text{O})_4\text{I}\cdot\text{S}$ (the sample had been washed and exchanged with ethanol) revealed a total weight loss of 17.86% up to 125 °C (Figure S2 in the SI) that could be attributed to the release of solvent water and ethanol molecules. A second step at 125–330 °C with 10.07% weight loss was due to the loss of coordinated DMSO and protonated water molecules. After that, the framework decomposed.

N_2 adsorption measurements were carried out at 77 K to investigate the permanent porosity of the framework, and its ability to adsorb H_2 and CO_2 was then studied. The as-synthesized products were first exchanged with dichloromethane and then heated at 100 °C for 24 h under high vacuum to obtain activated samples. The stability of the activated framework has been verified by powder X-ray diffraction data (Figure S3 in the SI). A reversible type I isotherm, with the characteristics of microporous materials, with maximal N_2 uptake of $309.2 \text{ cm}^3 \text{ g}^{-1}$ at 1 atm (Figure S4 in the SI) is observed, giving a Langmuir surface area of $1334.6 \text{ m}^2 \text{ g}^{-1}$ and a Brunauer–Emmett–Teller surface area of $1012.6 \text{ m}^2 \text{ g}^{-1}$, respectively. The adsorption of H_2 at 77 K is estimated to be $152.7 \text{ cm}^3 \text{ g}^{-1}$ or 1.38 wt % at 1 atm (Figure 2a), a bit larger than that of MOF-5 ($127 \text{ cm}^3 \text{ g}^{-1}$). The CO_2 uptake capacities (at 1 atm) are 84.3 and $58.1 \text{ cm}^3 \text{ g}^{-1}$ at 273 and 297 K, respectively (Figure 2a). At zero loading, the enthalpy of CO_2 adsorption ($-Q_{\text{st}}$) is 25.7 kJ mol^{-1} , as estimated from the

sorption isotherms at 273 and 297 K using the virial equation (Figure S6 in the SI).¹⁶

We further investigated its uptake capacity for light hydrocarbons (Figure 2b). The maximal sorption values at ambient pressures for pure CH_4 , C_2H_2 , C_2H_4 , and C_2H_6 are 19.5, 87.5, 62.5, and $67.1 \text{ cm}^3 \text{ g}^{-1}$ at 273 K and 13.0, 64.1, 43.4, and $53.8 \text{ cm}^3 \text{ g}^{-1}$ at 297 K, respectively. The adsorption heats are calculated to be 17.6, 29.4, 27.3, and 28.6 kJ mol^{-1} for CH_4 , C_2H_2 , C_2H_4 , and C_2H_6 , respectively (Figure S8 in the SI). Apparently, this MOF exhibits adsorption capacity following an order of $\text{C}_2\text{H}_2 > \text{C}_2\text{H}_4 \approx \text{C}_2\text{H}_6 > \text{CH}_4$, which has also been found in a Ni_4 -based MOF.^{7c} To evaluate its separation ability for light hydrocarbons, we calculated the sorptive selectivity of C_2 hydrocarbons over CH_4 using Henry's law (Table S3 and Figure S7 in the SI) based on equation $S_{i/j} = K_{\text{H}}(i)/K_{\text{H}}(\text{CH}_4)$. The results show that the selectivities for C_2H_2 , C_2H_4 , and C_2H_6 over CH_4 , respectively, are 25.0, 15.0, and 27.7 at 273 K and 16.3, 10.7, and 18.4 at 297 K, which are much higher than those of materials ZJU-48a (ionic MOF)^{16a} and UTSA-36a^{16b} with nearly equal adsorption quantity. Alternatively, the calculations using the ideal adsorbed solution theory¹⁷ give the sorptive selectivities for C_2H_2 , C_2H_4 , and C_2H_6 over CH_4 under 100 kPa as 22.6, 12.3, and 19.3 at 273 K and 14.1, 9.2, and 13.8 at 297 K, respectively (Figure S9 in the SI). It should be noticed that, although the adsorption heats are lower than those of MOFs with high-density open-metal sites (M-MOF-74, where M = Mg, Co, Fe) and HKUST-1, the $\text{C}_2\text{H}_6/\text{CH}_4$ selectivity at 297 K is comparable to that of MOF-74.^{3,18} This result implies that the present MOF may be a good candidate material for the separation of C_2H_6 over CH_4 .

Direct-current magnetic susceptibility of $(\text{H}_3\text{O})_4\text{I}\cdot\text{S}$ was collected at the 2–300 K temperature range, and the $\chi_{\text{M}}T$ versus T plot is shown in Figure 3. The $\chi_{\text{M}}T$ value at room temperature

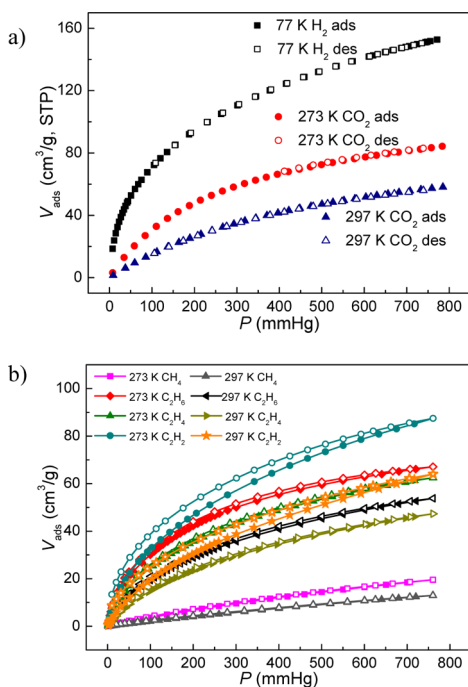


Figure 2. Adsorption (full symbols) and desorption (empty symbols) isotherms of H_2 and CO_2 (a) and C_2H_2 , C_2H_4 , C_2H_6 , and CH_4 (b).

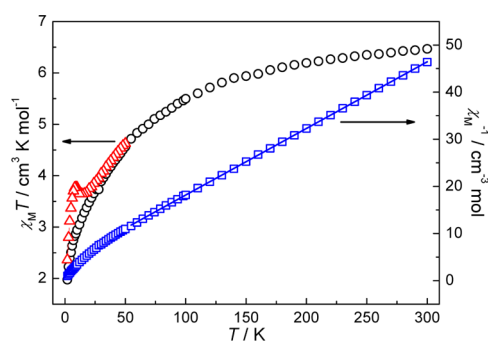


Figure 3. $\chi_{\text{M}}T$ versus T plot (per Ni^{II} unit) under applied fields of 1000 Oe (black) and 50 Oe (red), respectively.

is $6.47 \text{ cm}^3 \text{ K mol}^{-1}$, which is slightly higher than that expected for six isolated spin-only nickel(II) ions ($S = 1$ and $g = 2.0$) and results in a realistic g_{Ni} value of 2.08. The $\chi_{\text{M}}T$ value monotonously decreases upon temperature cooling, attaining $1.97 \text{ cm}^3 \text{ K mol}^{-1}$ at 2 K. The χ_{M}^{-1} versus T data above 50 K are fitted with the Curie–Weiss law to give a Weiss temperature of -28.62 K , thus clearly indicating an overall antiferromagnetic nature within the Ni_6^{II} unit (interunit magnetic interactions are negligible). On the other hand, isothermal magnetization at 2 K equals $3.97 \text{ N}\beta$ at 5 T (Figure S10 in the SI) that is much lower than the theoretical saturation value for a Ni_6^{II} unit ($12 \text{ N}\beta$ with $g = 2.0$), further confirming the antiferromagnetic properties of the Ni_6^{II} unit.

Interestingly, the magnetic susceptibility shows field-dependent behavior at temperatures below 25 K (Figure 3, red). Under

an applied magnetic field of 50 Oe, the magnetic susceptibility shows an upsurge at 9 K that is most probably attributed to the spontaneous magnetization of spin canting.^{7c,19} A narrow magnetic hysteresis loop was indeed observed with a coercive field of 33 Oe and a remnant magnetization of 0.008 N β , respectively (Figure S11 in the SI), and the canting angle can be estimated to be 0.04° based on the equation $\alpha = \tan^{-1}(M_r/M_s)$. Hence, this complex can be viewed as a weak ferromagnetic material. Moreover, field-cooled (FC) and zero-field-cooled (ZFC) magnetizations measured at 50 Oe in the 2–20 K temperature range diverge below 12 K (Figure S12 in the SI), suggesting an onset of ferromagnetic ordering. Because the framework structure is highly symmetric and the Ni^{II}₆ unit possesses a 2-fold-symmetric axis/plane between Ni1/Ni1a...Ni2 and Ni1...Ni1b (Figure 1a) so that antisymmetric magnetic interactions cannot be realized. Otherwise, the single-ion magnetic anisotropy of nickel(II) that has been revealed by the nonzero magnetic susceptibility at extremely low temperature (1.97 cm³ K mol⁻¹ at 2 K) and the realistic g_{Ni} value (2.08) should be the key point contributed to the occurrence of spin canting.

In conclusion, we have presented an anionic MOF constructed with a new hexanuclear nickel(II) unit and a trigonal-planar ligand. Although being 2-fold interpenetrated, this MOF shows the capability to adsorb H₂, CO₂, and light hydrocarbons, and most important is that it exhibits high separation selectivity of C₂H₂, C₂H₄, and C₂H₆ over CH₄. On the other hand, spin canting and a magnetic hysteresis loop revealed by magnetic studies indicate weak ferromagnetism in this complex.

■ ASSOCIATED CONTENT

■ Supporting Information

X-ray crystallographic data in CIF format, materials, synthetic details, TGA, IR, crystallographic data, and supplementary tables and figures. This material is available free of charge via the Internet at <http://pubs.acs.org>.

■ AUTHOR INFORMATION

Corresponding Author

*E-mail: taojun@xmu.edu.cn.

Notes

The authors declare no competing financial interest.

■ ACKNOWLEDGMENTS

This work was supported by the National Natural Science Foundation of China (Grant 21325103) and the National Key Basic Research Program of China (973 Project, Grant 2014CB845601).

■ REFERENCES

- (1) (a) Murray, L. J.; Dincă, M.; Long, J. R. *Chem. Soc. Rev.* **2009**, 38, 1294–1314. (b) Bux, H.; Liang, F.-Y.; Li, Y.-S.; Cravillon, J.; Wiebcke, M.; Caro, J. J. *Am. Chem. Soc.* **2009**, 131, 16000–16001.
- (2) (a) Zhou, H.-C.; Long, J. R.; Yaghi, O. M. *Chem. Rev.* **2012**, 112, 673–674. (b) Li, J.-R.; Ma, Y.; McCarthy, M. C.; Sculley, J.; Yu, J.; Jeong, H.-K.; Balbuena, P. B.; Zhou, H.-C. *Coord. Chem. Rev.* **2011**, 255, 1791–1823. (c) Li, J.-R.; Kuppler, R. J.; Zhou, H.-C. *Chem. Soc. Rev.* **2009**, 38, 1477–1504.
- (3) (a) Xiang, S.-C.; He, Y.-B.; Zhang, Z.-J.; Wu, H.; Zhou, W.; Krishna, R.; Chen, B.-L. *Nat. Commun.* **2012**, 3, 954–962. (b) He, Y.-B.; Zhou, W.; Yildirim, T.; Chen, B.-L. *Energy Environ. Sci.* **2013**, 6, 2735–2744.
- (4) (a) Zheng, S.-T.; Bu, J. T.; Li, Y.; Wu, T.; Zuo, F.; Feng, P.; Bu, X. J. *Am. Chem. Soc.* **2010**, 132, 17062–17064. (b) Lin, Q.; Wu, T.; Zheng, S.-T.; Bu, X.; Feng, P. J. *Am. Chem. Soc.* **2012**, 134, 784–787. (c) Liao, P.-Q.; Zhou, D.-D.; Zhu, A.-X.; Jiang, L.; Lin, R.-B.; Zhang, J.-P.; Chen, X.-M. *J. Am. Chem. Soc.* **2012**, 134, 17380–17383.
- (5) (a) Eerenstein, W.; Mathur, N. D.; Scott, J. F. *Nature* **2006**, 442, 759–765. (b) Singh, M. K.; Yang, Y.; Takoudis, C. G. *Coord. Chem. Rev.* **2009**, 253, 2920–2934.
- (6) (a) Rogez, G.; Viart, N.; Drillon, M. *Angew. Chem., Int. Ed.* **2010**, 49, 1921–1923. (b) Cui, H.-B.; Wang, Z.-M.; Takahashi, K.; Okano, Y.; Kobayashi, H.; Kobayashi, A. J. *Am. Chem. Soc.* **2006**, 128, 15074–15075.
- (7) (a) Halder, G. J.; Kepert, C. J.; Moubaraki, B.; Murray, K. S.; Cashion, J. D. *Science* **2002**, 298, 1762–1765. (b) Neville, S. M.; Halder, G. J.; Chapman, K. W.; Duriska, M. B.; Moubaraki, B.; Murray, K. S.; Kepert, C. J. *J. Am. Chem. Soc.* **2009**, 131, 12106–12108. (c) Li, J.; Guo, Y.; Fu, H.-R.; Zhang, J.; Huang, R.-B.; Zheng, L.-S.; Tao, J. *Chem. Commun.* **2014**, 50, 9161–9164.
- (8) (a) Li, Y.-W.; Li, J.-R.; Wang, L.-F.; Zhou, B.-Y.; Chen, Q.; Bu, X.-H. *J. Mater. Chem. A* **2013**, 1, 495–499. (b) Tong, X.-L.; Hu, T.-L.; Zhao, J.-P.; Wang, Y.-K.; Zhang, H.; Bu, X.-H. *Chem. Commun.* **2010**, 46, 8543–8545.
- (9) Wang, C.-F.; Li, R.-F.; Chen, X.-Y.; Wei, R.-J.; Zheng, L.-S.; Tao, J. *Angew. Chem., Int. Ed.* **2015**, 54, 1574–1577.
- (10) (a) McDonald, T. M.; Lee, W. R.; Mason, J. A.; Wiers, B. M.; Hong, C. S.; Long, J. R. *J. Am. Chem. Soc.* **2012**, 134, 7056–7065. (b) Vaidhyanathan, R.; Iremonger, S. S.; Shimizu, G. K. H.; Boyd, P. G.; Alavi, S.; Woo, T. K. *Science* **2010**, 330, 650–653. (c) Du, L.-T.; Lu, Z.-Y.; Zheng, K.-Y.; Wang, J.-Y.; Zheng, X.; Pan, Y.; You, X.-Z.; Bai, J.-F. *J. Am. Chem. Soc.* **2013**, 135, 562–565.
- (11) (a) Chen, S.; Zhang, J.; Wu, T.; Feng, P.; Bu, X. J. *Am. Chem. Soc.* **2009**, 131, 16027–16029. (b) Zhai, Q.-G.; Lin, Q.; Wu, T.; Wang, L.; Zheng, S.-T.; Bu, X.; Feng, P. *Chem. Mater.* **2012**, 24, 2624–2626. (c) Procopio, E. Q.; Linares, F.; Montoro, C.; Colombo, V.; Maspero, A.; Barea, E.; Navarro, J. A. R. *Angew. Chem., Int. Ed.* **2010**, 49, 7308–7311.
- (12) (a) Peralta, D.; Chaplais, G.; Simon-Masseron, A.; Barthelet, K.; Chizallet, C.; Quoineaud, A.-A.; Pirngruber, G. D. *J. Am. Chem. Soc.* **2012**, 134, 8115–8126. (b) Park, H. J.; Suh, M. P. *Chem. Sci.* **2013**, 4, 685–690.
- (13) (a) Sun, D.-F.; Ma, S.-Q.; Ke, Y.-X.; Collins, D. J.; Zhou, H.-C. *J. Am. Chem. Soc.* **2006**, 128, 3896–3897. (b) Ma, S.-Q.; Zhou, H.-C. *J. Am. Chem. Soc.* **2006**, 128, 11734–11735. (c) Ma, S.-Q.; Sun, D.-F.; Ambrogio, M. W.; Fillinger, J. A.; Parkin, S.; Zhou, H.-C. *J. Am. Chem. Soc.* **2007**, 129, 1858–1859. (d) Li, J.; Huang, P.; Wu, X.-R.; Tao, J.; Huang, R.-B.; Zheng, L.-S. *Chem. Sci.* **2013**, 4, 3232–3238.
- (14) (a) Sun, D.-F.; Ma, S.-Q.; Ke, Y.-X.; Petersen, T. M.; Zhou, H.-C. *Chem. Commun.* **2005**, 2663–2665. (b) Sun, D.-F.; Ke, Y.-X.; Collins, D. J.; Lorigan, G. A.; Zhou, H.-C. *Inorg. Chem.* **2007**, 46, 2725–2734.
- (15) (a) Zhang, X.-M.; Zheng, Y.-Z.; Li, C.-R.; Zhang, W.-X.; Chen, X.-M. *Cryst. Growth Des.* **2007**, 7, 980–983. (b) Zheng, Y.-Z.; Tong, M.-L.; Xue, W.; Zhang, W.-X.; Chen, X.-W.; Grandjean, F.; Long, G. J. *Angew. Chem., Int. Ed.* **2007**, 46, 6076–6080.
- (16) (a) Xu, H.; Cai, J.-F.; Xiang, S.-C.; Zhang, Z.-J.; Wu, C.-D.; Rao, X.-T.; Cui, Y.-J.; Yang, Y.; Krishna, R.; Chen, B.-L.; Qian, G.-D. *J. Mater. Chem. A* **2013**, 1, 9916–9921. (b) Das, M. C.; Xu, H.; Xiang, S.-C.; Zhang, Z.-J.; Arman, H. D.; Qian, G.-D.; Chen, B.-L. *Chem.—Eur. J.* **2011**, 17, 7817–7822.
- (17) Myers, A. L.; Prausnitz, J. M. *AIChE J.* **1965**, 11, 121–127.
- (18) (a) Bae, Y.-S.; Lee, C. Y.; Kim, K. C.; Farha, O. K.; Nickias, P.; Hupp, J. T.; Nguyen, S. T.; Snurr, R. Q. *Angew. Chem., Int. Ed.* **2012**, 51, 1857–1860. (b) Bloch, E. D.; Queen, W. L.; Krishna, R.; Zadrozny, J. M.; Brown, C. M.; Long, J. R. *Science* **2012**, 335, 1606–1610. (c) Caskey, S. R.; Wong-Foy, A. G.; Matzger, A. J. *J. Am. Chem. Soc.* **2008**, 130, 10870–10871.
- (19) Li, J.; Tao, J.; Huang, R.-B.; Zheng, L.-S. *Inorg. Chem.* **2012**, 51, 5988–5990.